

Analysis of synchrotron radiation spectra of runaway electrons in Tokamak

M. Xiao, R. J. Zhou, L. Q. Hu, Y. K. Zhang, and EAST Team

Citation: *Physics of Plasmas* **24**, 124504 (2017); doi: 10.1063/1.5009772

View online: <https://doi.org/10.1063/1.5009772>

View Table of Contents: <http://aip.scitation.org/toc/php/24/12>

Published by the [American Institute of Physics](#)

Articles you may be interested in

[Lifetime and universal distribution of seed runaway electrons](#)

Physics of Plasmas **24**, 112509 (2017); 10.1063/1.5001931

[Magnetized electron emission from a small spherical dust grain in fusion related plasmas](#)

Physics of Plasmas **24**, 124502 (2017); 10.1063/1.4997695

[Self-organized criticality in a cold plasma](#)

Physics of Plasmas **24**, 120701 (2017); 10.1063/1.5005560

[Theory and observation of the onset of nonlinear structures due to eigenmode destabilization by fast ions in tokamaks](#)

Physics of Plasmas **24**, 122508 (2017); 10.1063/1.5007811

[One-dimensional particle simulation of wave propagation and generation of second harmonic waves in a composite of plasma and metamaterial](#)

Physics of Plasmas **24**, 122112 (2017); 10.1063/1.5001108

[Effect of lower hybrid current drive on pedestal instabilities in the HL-2A tokamak](#)

Physics of Plasmas **24**, 122507 (2017); 10.1063/1.5009509



**COMPLETELY
REDESIGNED!**



**PHYSICS
TODAY**

Physics Today Buyer's Guide
Search with a purpose.

Analysis of synchrotron radiation spectra of runaway electrons in Tokamak

M. Xiao,^{1,2} R. J. Zhou,^{1,a)} L. Q. Hu,¹ Y. K. Zhang,¹ and EAST Team¹

¹Institute of Plasma Physics, Chinese Academy of Sciences, Hefei 230031, China

²University of Chinese Academy of Sciences, Beijing 100049, China

(Received 19 October 2017; accepted 29 November 2017; published online 13 December 2017)

The full expression of runaway electron radiation in a tokamak is calculated accurately without any additional simplifications in this letter. By comparing the synchrotron radiation spectra of runaway electrons based on the full expression, their asymptotic expressions, and pure circular orbit expressions, it is analyzed how radiation spectra and total radiation power of runaway electrons in Tokamak can be analyzed correctly and efficiently. *Published by AIP Publishing.*

<https://doi.org/10.1063/1.5009772>

Detection of the synchrotron radiation emitted by runaway electrons in a tokamak has been claimed as an effective and powerful measurement to diagnose high energy runaway electrons directly in the core of plasma.^{1–3} It is the most essential way to analyse the synchrotron spectra from runaway electrons correctly. The aim of this work is to study if the synchrotron spectra of runaway electrons can be analyzed correctly and efficiently at the same time, when runaway electrons in the Tokamak can be treated by a pure circular orbit.

The spectral density of the power emitted by an electron moving along a circular orbit with Lorentz factor $\gamma \gg 1$ at wavelength λ is well known as⁴

$$\frac{dP(\lambda)}{d\lambda} = \frac{1}{\sqrt{3}} \frac{ce^2}{\epsilon_0 \lambda^3 \gamma^2} \int_w^\infty K_{5/3}(x) dx, \quad (1)$$

where $w = 4\pi R_{curv}/3\lambda\gamma^3$, R_{curv} is the instantaneous radius of curvature of the electron orbit with $1/R_{curv} = |\dot{\mathbf{r}} \times \ddot{\mathbf{r}}/\dot{\mathbf{r}}|^3$, and \mathbf{r} is the position vector of the electron. The motion of electrons in tokamak plasma is a superposition of their guiding center motion that follows the helicity of the magnetic field lines, cyclotron gyration motion around the guiding center with frequency $\omega_{ce} = eB/m_e\gamma$, and vertical centrifugal drift motion with velocity $v_{dr} = (v_{\parallel}^2 + v_{\perp}^2/2)/\omega_{ce}R_0 \approx v_{\parallel}^2/(\omega_{ce}R_0)$ due to the curvature and gradient magnetic field drifts. So, actually the radiation from high energy runaway electrons is the synchro-curvature radiation.⁵ In this case, the instantaneous curvature radius of the electron orbit depends on the phase of cyclotron gyration and it will oscillate strongly⁶

$$\frac{1}{R_{curv}^2} \approx \frac{1}{R_0^2} [1 + \eta^2 + 2\eta \sin(\bar{\theta} + \bar{\alpha})], \quad (2)$$

where $\eta = v_{\perp}/v_{dr} \approx eBR_0\theta_p/m_e c\gamma$, with $\theta_p = \arctan(v_{\perp}/v_{\parallel})$ being the pitch angle. When the value of the pitch angle is small, the approximation $\theta_p = \arctan(v_{\perp}/v_{\parallel}) \approx v_{\perp}/v_{\parallel}$ stands. θ is the poloidal angle corresponding to the position of the electron guiding center and α is the cyclotron gyration phase with $\dot{\alpha} \approx -\omega_{ce}$. The overhead bar stands for the

averaging over the period of cyclotron gyration. It is possible to introduce an averaged spectral density of the emitted power⁶

$$\begin{aligned} \frac{dP_{full}(\lambda)}{d\lambda} = & i \frac{ce^2}{2\epsilon_0 \lambda^3 \gamma^2} \left\{ \int_C \frac{du}{u} (1 - 2u^2) I_0 \left(\frac{\xi \eta u^3}{1 + \eta^2} \right) \right. \\ & \times \exp \left[-\frac{3}{2} \xi \left(u - \frac{u^3}{3} \right) \right] - \frac{4\eta}{1 + \eta^2} \int_C du u I_1 \left(\frac{\xi \eta u^3}{1 + \eta^2} \right) \\ & \left. \times \exp \left[-\frac{3}{2} \xi \left(u - \frac{u^3}{3} \right) \right] \right\}, \quad (3) \end{aligned}$$

where $\xi = 4\pi R_0/3\lambda\gamma^3 \sqrt{1 + \eta^2}$, and the integration path is an arbitrary contour running from an infinitely remote point in the sector $-\pi/2 < \arg u < -\pi/6$ to an infinitely remote point in the complex conjugate sector.

The integrands in Eq. (3) are highly oscillatory and the calculation of synchrotron spectra can become computationally heavy. The asymptotic approximation of Eq. (3) can simplify the spectra analysis by the saddle point method when $\xi \gg 1$. Two limit cases are possible.⁶ In the first case, when $\xi\eta/(1 + \eta^2) \leq 1$, the asymptotic expression of Eq. (3) will be

$$\begin{aligned} \frac{dP_{as1}(\lambda)}{d\lambda} \approx & \frac{ce^2}{4\epsilon_0} \sqrt{\frac{2\sqrt{1 + \eta^2}}{\lambda^5 R_0 \gamma}} \left[I_0(a) + \frac{4\eta}{1 + \eta^2} I_1(a) \right] \\ & \times \exp \left(-\frac{4\pi R_0}{3\lambda\gamma^3 \sqrt{1 + \eta^2}} \right). \quad (4) \end{aligned}$$

In the second case, when $4\pi R_0\eta/3\lambda\gamma^3(1 + \eta^2)^3 > 1$, the asymptotic expression of Eq. (3) will be

$$\begin{aligned} \frac{dP_{as2}(\lambda)}{d\lambda} \approx & \frac{\sqrt{3}ce^2\gamma}{8\pi\epsilon_0\lambda^2 R_0} \frac{(1 + \eta^2)^2}{\sqrt{\eta}} \\ & \times \exp \left(-\frac{4\pi R_0}{3\lambda\gamma^3(1 + \eta^2)} \right). \quad (5) \end{aligned}$$

Conditions that are required to ensure the validity of P_{as1} and P_{as2} should be analyzed before these two asymptotic expressions are used.⁷ Meanwhile, without any additional simplifications, P_{full} can be calculated accurately by

^{a)}Electronic mail: rjzhou@ipp.ac.cn

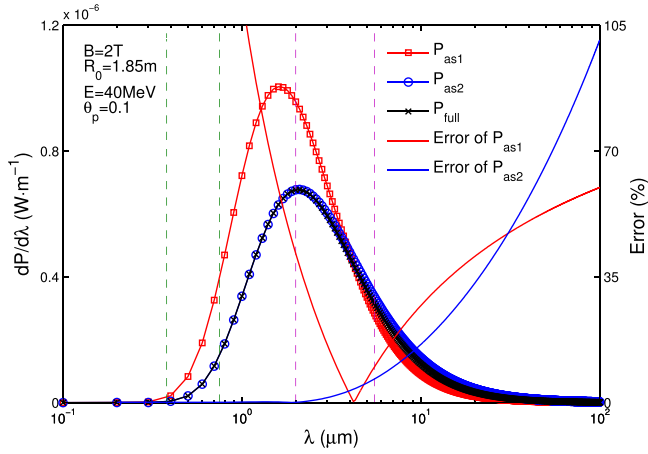


FIG. 1. Comparison of synchrotron radiation spectra of runaway electrons based on the full expression Eq. (3), and its asymptotic expressions Eqs. (4) and (5), with typical EAST parameters. The errors of Eqs. (4) and (5) to Eq. (3) are also given. The ranges of visible (0.38–0.75 μm) and infrared (2–5.5 μm) light are labeled by the green and pink dashed lines, respectively.

integrating Eq. (3) in the complex plane, although the computation is much heavier than P_{as1} and P_{as2} .

The comparison of synchrotron radiation spectra of runaway electrons based on Eq. (3), and their asymptotic expressions Eqs. (4) and (5), with typical EAST parameters is given in Fig. 1. The error of asymptotic expressions is given by $|P_{as} - P_{full}|/P_{full}$. The ranges of visible and infrared light are selected according to the typical sensitive wavelength of the visible and infrared cameras used. It indicates that P_{as2} is a good asymptotic expression in EAST, with $|P_{as2} - P_{full}|/P_{full} < 10\%$ in both wavelength ranges; However, the error of P_{as2} increases greatly as the wavelength increases, which will cause a large error when the total radiation power of runaway electrons is calculated.

Now, we analyze the errors of asymptotic expressions Eqs. (4) and (5) to full expression Eq. (3) in a wider parameter range based on the achievable experimental conditions in EAST. In Fig. 2, four electron energies E (a) and four pitch angles θ_p (b) are analyzed. It is not a linear relationship between errors and energies or pitch angles. When $E=40\text{ MeV}$ and $\theta_p=0.1$, the error of P_{as2} to P_{full} is at its minimum. Still, $|P_{as2} - P_{full}|/P_{full} < 20\%$ in both wavelength ranges can be guaranteed in all the parameter ranges. Moreover, in the parameter ranges of magnetic field B (1.8–2.4 T) and major radius of the magnetic surface R_0 (1.82–1.91 m), the errors of these two asymptotic expressions do not change greatly.

ITER is a tokamak with a much larger size and higher magnetic field than EAST. Situations in ITER will be particularly interesting. The comparison of synchrotron radiation spectra of runaway electrons based on Eq. (3), and their asymptotic expressions Eqs. (4) and (5) with typical ITER parameters is given in Fig. 3. It indicates that P_{as2} has a smaller error in the visible light range, however, the error increases greatly from 0.38 μm to 0.75 μm , which makes it hard to correct this error in the integral data of visible camera. P_{as1} is better than P_{as2} in the infrared light range, but the error is already very large now. So, neither P_{as1} nor P_{as2} is good enough to approximate P_{full} in this ITER condition, and

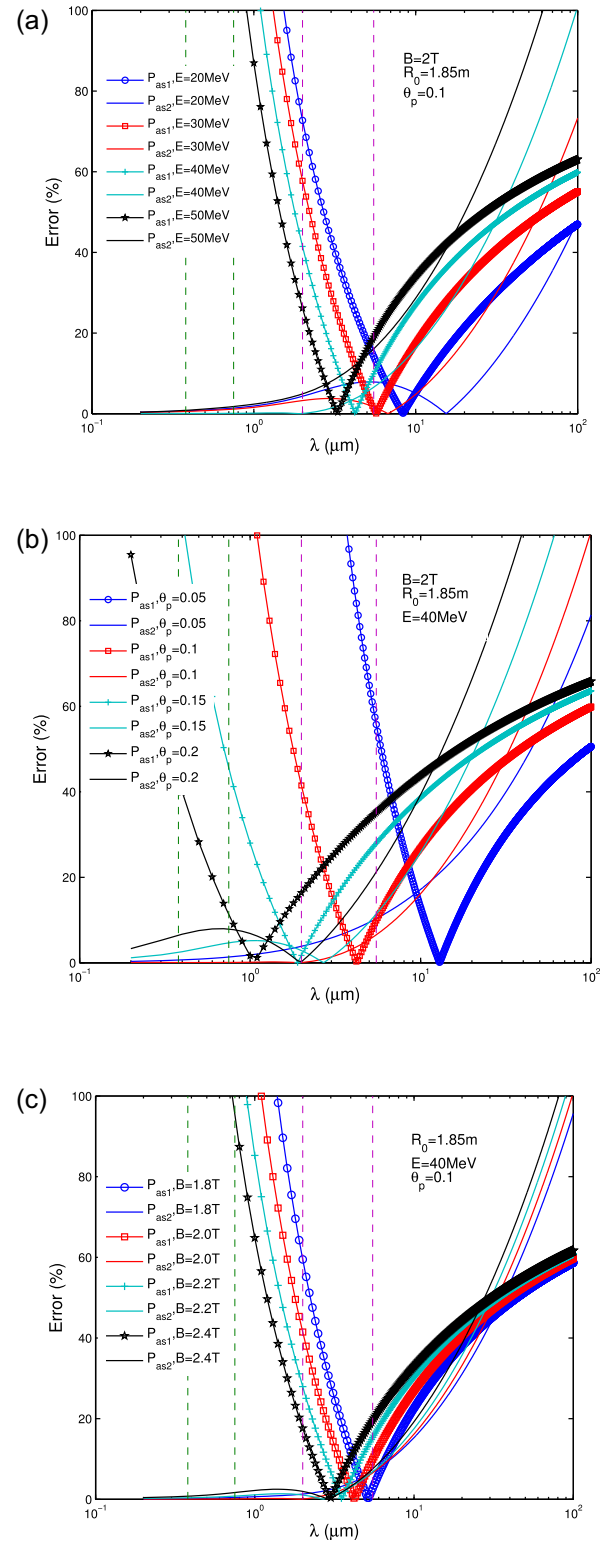


FIG. 2. Errors of the asymptotic expressions Eqs. (4) and (5) to full expression Eq. (3), with typical EAST parameters. Four electron energies E (a), four pitch angles θ_p (b), and four magnetic fields (c) are analyzed.

it is better to use P_{full} all the time. Meanwhile, it shows that abundant synchrotron radiation from runaway electrons will fall into the visible light range in ITER. It is much easier to obtain a fast response with a visible camera than an infrared camera, which means it will be favorable to study the dynamics of runaway electrons.

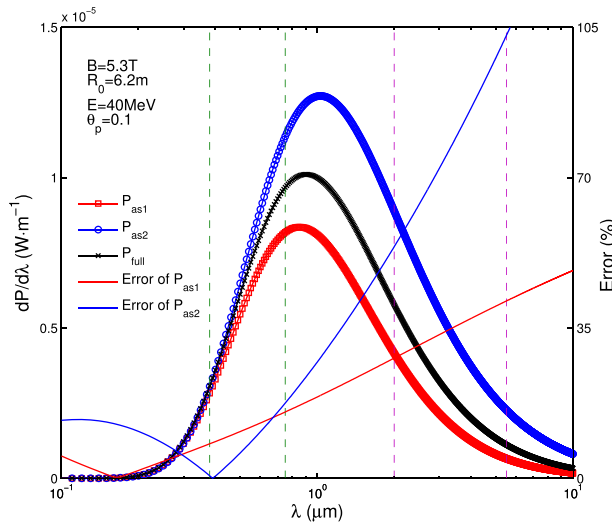


FIG. 3. Comparison of synchrotron radiation spectra of runaway electrons based on Eq. (3), and their asymptotic expressions Eqs. (4) and (5), with typical ITER parameters.

Finally, it is very important to estimate the total radiation power of runaway electrons in the tokamak, since runaway electrons can lose large amounts of energies through their synchrotron radiation.

We consider that the parameter η indicates the extent of changing the curvature radius along the particle trajectory, which can determine the radiation mode of runaway electrons.^{8,9} The full expression Eq. (3) should approach the pure curvature radiation in the limit $\eta \rightarrow 0$ and approach the pure synchrotron radiation in the limit $\eta \rightarrow \infty$. So, the total radiation power of runaway electrons $P = \int_{\lambda} (dP/d\lambda) d\lambda$ in several tokamaks with the relationship of parameter η analyzed, as shown in Fig. 4. Beside those 6 tokamaks, parameters $B=10$ T and $R_0=1$ m are used to approach the curvature radiation, and parameters $B=1$ T and $R_0=10$ m are used to approach the synchrotron radiation, to understand the nature of this physical process.

Four expressions are estimated: pure circular orbit expression Eq. (1) (labeled as P_{circle} in Fig. 4), full expression Eq. (3), and asymptotic expressions Eqs. (4) and (5). It indicates that the total radiation power of runaway electrons in the tokamak is located in the middle of pure curvature and pure synchrotron radiation, and runaway electrons in most tokamaks exhibit the feature closer to pure synchrotron radiation. Alcator C-Mod is a tokamak with a very high magnetic field but a small major radius, so, runaway electrons in this tokamak exhibit the feature closer to pure curvature radiation instead.

The errors of total radiation power based on Eqs. (1), (4), and (5) to Eq. (3) are also given. It can be seen that the error of P_{circle} decreases along with the increase of η , which is due to the fact that the full expression Eq. (3) approaches the pure synchrotron radiation in the limit $\eta \rightarrow \infty$. So, P_{circle} can be used in ITER to estimate the total radiation power of runaway electrons with error $|P_{as2} - P_{full}|/P_{full} < 10\%$. Whereas, it will cause a very large error in the EAST case, if P_{circle} is used. In the EAST case, P_{as1} is better than P_{as2} to estimate the total radiation power, with error $|P_{as1} - P_{full}|/P_{full} < 5\%$.

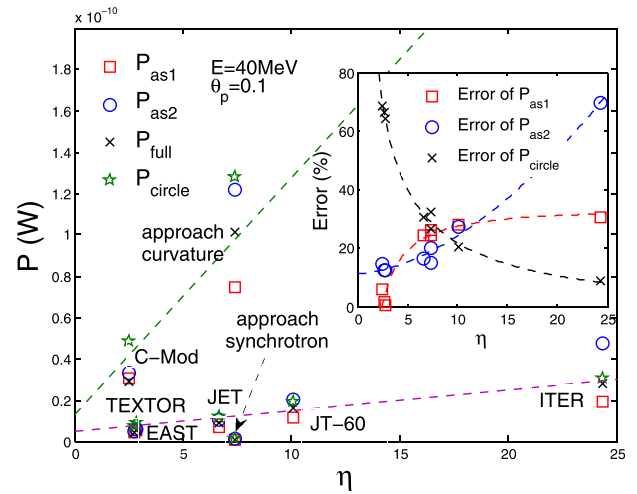


FIG. 4. The total radiation power of runaway electrons ($E=40$ MeV and $\theta_p=0.1$) in several tokamaks with the relationship of parameter η , estimated by four expressions: pure circular orbit expression Eq. (1), full expression Eq. (3), and its asymptotic expressions Eqs. (4) and (5). The errors of Eqs. (1), (4), and (5) to Eq. (3) are also given.

In summary, the full expression of runaway electron radiation P_{full} can be calculated accurately without any additional simplifications but with a much heavier computation.

When the radiation spectra of runaway electrons are analyzed, P_{as2} is a good asymptotic expression in EAST, with $|P_{as2} - P_{full}|/P_{full} < 10\%$ in both the visible and infrared wavelength range, and neither P_{as1} nor P_{as2} is good enough to approximate P_{full} in the ITER condition, and it is better to use P_{full} all the time.

The total radiation power of runaway electrons is located in the middle of pure curvature and pure synchrotron radiation, and runaway electrons in most tokamaks exhibit the feature closer to pure synchrotron radiation. To estimate the total radiation power of runaway electrons, P_{as1} is better than P_{as2} with error $|P_{as1} - P_{full}|/P_{full} < 5\%$ in EAST to simplify the calculation, and P_{circle} can be used in ITER with error $|P_{as2} - P_{full}|/P_{full} < 10\%$.

The authors would like to thank Professor I. M. Pankratov (NSC KIPT, Ukraine) for the helpful discussions in understanding synchrotron radiation equations of runaway electrons in tokamaks. This work was supported by the National Natural Science Foundation of China under Grant Nos. 11775263 and 11405219, and was partially supported by the JSPS-NRF-NSFC A3 Foresight Program in the field of Plasma Physics (NSFC No. 11261140328).

¹K. Finken, J. Watkins, D. Rusbüldt, W. Corbett, K. Dippel, D. Goebel, and R. Moyer, *Nucl. Fusion* **30**, 859 (1990).

²R. Jaspers, N. Lopes Cardozo, A. Donne, H. Widdershoven, and K. Finken, *Rev. Sci. Instrum.* **72**, 466 (2001).

³A. Stahl, M. Landreman, G. Papp, E. Hollmann, and T. Fulop, *Phys. Plasmas* **20**, 093302 (2013).

⁴J. Schwinger, *Phys. Rev.* **75**, 1912 (1949).

⁵K. Cheng and J. Zhang, *Astrophys. J.* **463**, 271 (1996).

⁶I. M. Pankratov, *Plasma Phys. Rep.* **25**, 145 (1999).

⁷R. J. Zhou, I. M. Pankratov, L. Q. Hu, M. Xu, and J. H. Yang, *Phys. Plasmas* **21**, 063302 (2014).

⁸Y. M. Sobolev, *Prob. Atomicity Technol.* **466**, 108 (2013).

⁹Y. M. Sobolev, *Polarization* **3**, 2 (2015).